

PERFORMANCE ASSESSMENT OF AN ENGINE-INTEGRATED CLOSED-AIR COOLING THERMAL MANAGEMENT SYSTEM IN A NEXT GENERATION FIGHTER CONFIGURATION

Tomasz Matuschek¹, Jannik Häßy¹, Marc Schmelcher¹ & Alexander Görtz¹

¹ German Aerospace Center (DLR), Linder Höhe, 51147 Köln, Germany

Abstract

The increasing integration of high-performance electronics into supersonic aircraft introduces a significant thermal challenge for aviation engineers. Future fighter aircraft are expected to manage heat in the megawatt range. This necessitates the implementation of an efficient thermal management system (TMS) capable of intelligent heat dissipation through the utilization of multiple heat sinks.

This paper investigates an engine-integrated TMS that utilizes engine airflow for heat dissipation. A closed-air reverse Brayton cycle is analyzed where heat is transferred from a coolant to the engine bypass flow. However, the operation of such a refrigeration cycle affects engine performance. For instance, it requires additional power from the engine, and the increased system mass necessitates a higher thrust demand. This study aims to analyze the trade-offs between cooling capacity and engine performance through an off-design analysis of a fighter configuration developed at the German Aerospace Center (DLR).

By presenting the study results, the aim is to elucidate the interrelations, benefits, and disadvantages, providing a comprehensive understanding of an engine-integrated closed-air cooling TMS. The knowledge gained can be used in future studies to conduct architectural assessments and further enhance the efficiency and potential of engine TMS solutions.

Keywords: thermal management system, engine performance, thermodynamics, refrigeration cycle

1. Introduction

In modern aviation, efficiently managing the heat generated by high-performance electronic systems poses an ever-growing challenge. This is particularly critical in future military applications, such as next-generation fighters, where the thermal load from these systems significantly impacts aircraft performance and safety [1,2]. This issue is further exacerbated for planned deployments of energy weapons due to their low efficiency of about 25 % [2]. It is expected that even with the use of advanced heat storage technologies, the level of heat to be dissipated will significantly increase, sometimes even reaching the MW range [3,4].

Traditional cooling technologies cannot be readily scaled up due to stricter aircraft requirements and technological constraints. For instance, ram-air ducts with openings on the aircraft's outer skin adversely affect external aerodynamics and have a detrimental impact on radar signature [3]. Fuel cooling systems face limitations related to maximum preheating temperatures and the decreasing amount of fuel during the flight [2].

The Air Force Research Laboratory (AFRL) launched the *Integrated Vehicle & Energy Technology* (INVENT) program, which addresses the thermal challenges of military platforms and develops and evaluates modern cooling technologies and efficient Thermal Management Systems (TMS). Some approaches that utilize engine air flows to assist in heat dissipation offer promising alternatives, yet also pose challenges regarding aircraft performance and fuel consumption. [5]

A notable example where an engine-integrated TMS is already employed is the F-35's Power and Thermal Management System (PTMS) developed by Honeywell [6]. However, it also illustrates the challenges of modern fighter aircraft. Despite these advanced systems, the F-35 encounters thermal limits following the enhancements in electronic warfare and target recognition (Block 4 upgrades),

PERFORMANCE ASSESSMENT OF AN ENGINE INTEGRATED CLOSED-AIR THERMAL MANAGEMENT SYSTEM

which constrain the jet's performance [7]. This situation even led to extensive discussions about developing a new propulsion system with higher cooling capabilities [8]. Although these considerations were ultimately dismissed due to technical complexity and costs [9], they underscore the necessity for future fighter designs to incorporate integrated TMS within the conceptual design phase, considering their impact on engine performance [10].

This paper will analyze the combination of a modern propulsion system with a closed-air cooling cycle – similar to the configuration of the F-35 PTMS. The focus will be less on a detailed design but more on the fundamental relationships, trade-offs, and potentials that such an engine-integrated TMS offers.

2. State of the art

Aircraft TMS cover a broad area, with ongoing intensive development due to the previously mentioned challenges. A review of the literature on TMS in aviation shows significant growth, with the number of annual publications increasing by a factor of five over the last 20 years. This is detailed in a comprehensive study by van Heerden et al. [3], which reviews current solutions for efficient heat dissipation and their various applications in aviation. Notably, studies on the integration of energy weapons into high-performance aircraft conclude that traditional cooling technologies are inadequate for their immense cooling requirements and suggest the use of innovative technologies such as vapor cycle systems and phase change materials as energy storage to handle peak heat loads [11-13]. These findings highlight the growing need for research and development beyond existing cooling technologies.

The integration of TMS into the engine and the application of bypass heat exchangers is a modern approach that has already been implemented. As mentioned before, Honeywell developed a PTMS for the F-35 that facilitates heat dissipation via the bypass duct in cooling mode. It utilizes components from the auxiliary power unit to drive a refrigeration cycle connected to a bypass heat exchanger [6]. Systems like these generally have a negative impact on engine performance, which must be weighed against the advantages of its heat dissipation capabilities. Unfortunately, detailed studies on the design and trade-off analysis for the PTMS and engine performance of the F-35 have not been published.

Nevertheless, there are some notable publications and examples of TMS designs being integrated into the conceptual design phase of military engines. Maser [14] introduced a design method focused on minimizing exergy losses, allowing for comparison between losses in propulsion and TMS. Clark et al. [15] used an existing environmental control system architecture to demonstrate the impact of design points on heat dissipation potential during off-design operation of a military fighter engine, similar to the F135 engine of the F-35. These studies are extended to include the design of a variable cycle engine with a second continuously flowing bypass channel [10,16]. However, it should be noted that the considered TMS represents an open-air system powered by bleed air, differing from the closed variant like it is used for the F-35's PTMS.

To identify efficient TMS solutions, it is necessary to evaluate and compare different system architectures. A review of the available literature indicates that there is a lack of analysis on the operational behavior of simple closed-air refrigeration cycles in combination with engine performance assessments for modern fighter configurations. These analyses could serve as a basis for further developments and would complement results such as those found in [10,15,16]. This paper aims to address this gap and provide a general understanding of closed-air TMS solutions utilizing bypass heat exchangers.

3. Methods and Tools

This study focuses on the fighter configuration developed in DLR's project *Diabolo*, in particular the *Future Fighter Demonstrator* (DLR-FFD) and its advanced engine developed in DLR's project *Future Fighter Engine Technologies* (FFE+). Within the scope of this study, an engine-integrated TMS in the form of a retrofit is to be analyzed on the basis of the given fighter configuration. The engine design will remain unchanged, but will be extended by a bypass heat exchanger as well as the engine TMS. The effects are evaluated by means of an off-design performance simulation in which the sizing flight mission is considered in a simplified manner. Following is a brief summary of the aircraft configuration, the associated propulsion system, and the assumptions used in the mission analysis.

3.1 Future Fighter Demonstrator (DLR-FFD)

The DLR-FFD is a virtual concept of a highly agile, supersonic, next-generation fighter aircraft, illustrated in Figure 1. It is a twin-engine, manned platform with a low infrared and radar signature. The aircraft is designed for a mission radius of 550 nautical miles using only internal fuel. The configuration (DLR-FFD V3.2.0 design) describes an aircraft with a wingspan of 14.8 m, an overall length of 20.3 m, and a total weight of 28.3 tons for the sizing Combat Air Patrol (CAP) mission. Detailed specifications on requirements, payload and flight performance can be found in [17].

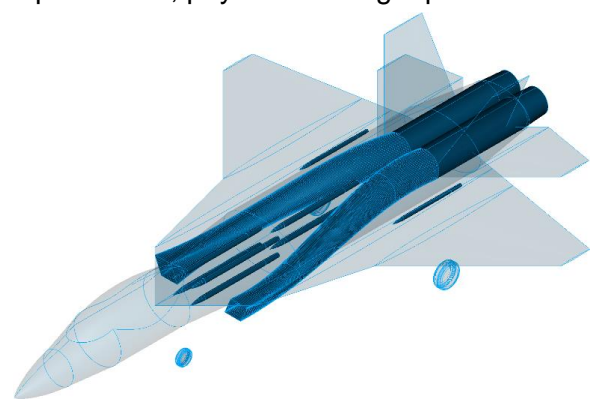


Figure 1 – DLR-FFD illustration with highlighted engines and intakes.

The design process utilizes the conceptual aircraft design software VAMPzeroF, calibrated and verified based on public data to ensure accuracy, especially as there is a lack of physics-based sizing methods that are applicable for conceptual aircraft design. The design integrates aircraft and engine requirements based on both constraint analysis and mission requirements, focusing on combat capabilities, flight extremes, and efficiency during long cruise and loiter phases for the sizing CAP mission. This approach ensures the engine performs optimally across various flight conditions while minimizing fuel consumption. The VAMPzeroF design process features three primary modules for analyzing performance constraints, computing mission requirements, and sizing systems. It begins with determining necessary thrust-to-weight ratios and wing loading from aircraft configurations and performance needs, progressing to mission-specific simulations for fuel and thrust requirements. This enables optimization for varied missions, essential for modern fighters. Higher fidelity aerodynamic and propulsion models enhance these analyses, feeding into a final sizing module that refines the aircraft's geometry and mass distribution iteratively for design convergence. [18]

3.2 Future Fighter Engine (DLR-FFE)

The DLR-FFE is a two-spool mixed turbofan engine equipped with an afterburner, assuming an advanced level of technology. The conceptual design of the engine is the result of a multidisciplinary design process developed at DLR, in which information is exchanged between the aircraft and engine design teams, allowing for internal optimization loops. The engine is sized based on the most demanding thrust requirements. Thermodynamic design parameters are optimized using aircraft sensitivities to quantify the engine's impact on the platform. Ultimately, this approach significantly reduces the number of global iterations between airframe and engine design. The methodology and detailed studies using the engine design process are presented in [19].

The propulsion system is simulated by means of the virtual engine platform Gas Turbine Laboratory (GTlab) developed at the Institute of Propulsion Technology (DLR-AT). The modular software architecture allows for a flexible simulation of aero engines and gas turbines at different levels of detail and features various integrated analysis tools [20]. The design of the DLR-FFE includes thermodynamic simulation, geometric predesign and engine mass estimation. The current version of the engine is the result of the fourth global iteration between aircraft and engine design, balancing the most demanding dry operating point (supercruise) with a wet, high-load maneuvering point [19]. The net thrust of the engine is 112.7 kN (177.1 kN wet) for take-off conditions with a fan diameter of 1 m, an overall length of approximately 5 m and an estimated weight of 1875 kg. The performance model and geometric predesign are shown in Figure 2. Since an advanced level of technology is assumed, high temperatures and pressure ratios occur, leading to challenging bypass temperatures up to 500 K, which adversely affects the engine's cooling performance.

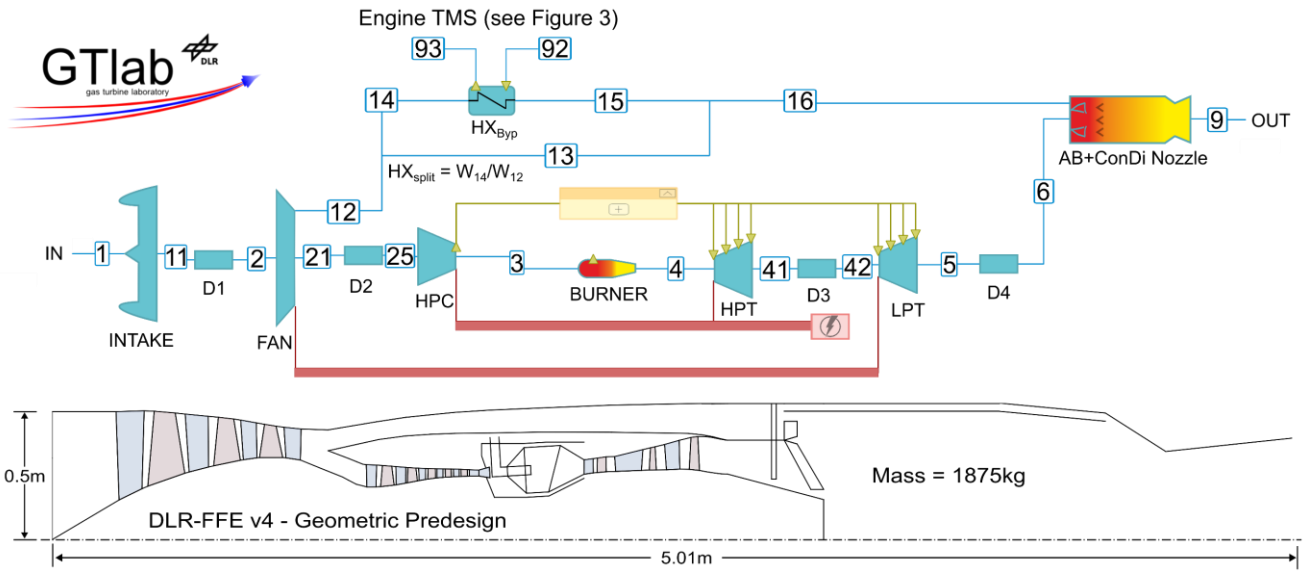


Figure 2 – thermodynamic performance model and geometric predesign of the DLR-FFE.

3.3 Flight Mission

The studies presented here analyze the aircraft sizing Combat Air Patrol flight mission. The mission involves patrolling over allied territory, with cruise and loiter phases punctuated by a supersonic air combat segment, emphasizing the need for efficiency due to the long cruise and loiter durations [17]. From the detailed flight mission simulation data provided by VAMPzeroF, operational points have been identified that accurately represent flight segments in terms of fuel burn and power levels. This allows the flight mission to be approximated with only a few off-design performance calculations, providing insight into fuel consumption throughout the mission. Notably, this approximation is also suitable for flight phases with changes in altitude and speed, such as climb. Further analysis of the data led to the use of defined thrust-to-weight ratios *T/W* at these operating points, rather than absolute thrust, accounting for fuel burned up to that point and linking directly to the propulsion system's efficiency. This method also allows consideration of additional weights, such as bypass heat exchangers. A summary of the flight mission segments and their representative operating points is given in Table 1.

T 11 1				
I ania 1 summai	1/ At tha 1 '/\ U tilAl	at miccian and	ranracantativa	Anaratina nainte
Table 1 – summar	V UI LIIG CAF IIIUI	il illissivii aliu	IGNIGOGIIIALIVG	UDGI ALII IU DUII ILS.

Combat Air Patrol (CAP) – starting aircraft mass 28,200 kg							
Segment	Altitude [m]	Ma [–]	Duration [s]	Distance [km]	req. Thrust		
Take-Off	0	0.19	26	1.5	max dry		
ClimbOut	6309	0.53	290	48.3	max dry		
CruiseOut	11000	0.85	3869	970.3	T/W = 0.43		
Patrol	10668	0.8	3600	854.0	T/W = 0.44		
Acceleration	11671	1.09	40	10.7	T/W = 2.77 (wet)		
Turn1	11671	1.21	68	24.2	T/W = 3.23 (wet)		
Turn2	10668	0.9	51	13.6	T/W = 2.98 (wet)		
Payload drop (-154 kg)							
ClimbIn	11482	0.9	300	79.9	T/W = 0.60		
CruiseIn	12192	0.9	3535	938.7	T/W = 0.50		

Technically, a decline in engine performance within a retrofit approach could lead to an unfeasible flight mission, necessitating a redesign of the aircraft. However, the design of the DLR-FFD has taken into account a fuel reserve to ensure the completion of the flight mission even with increased fuel burn. Therefore, the drawbacks of the engine TMS can be quantified by the additional fuel

required from the reserve. Furthermore, the DLR-FFD has allocated a certain amount of installation space for existing electrical systems, even if these have not been specified in detail. As a result, it can be assumed that the required installation space for the engine-integrated TMS is available within the configuration, and a redesign is not deemed necessary.

4. Thermal Management System Model

The considered engine-integrated TMS is a simple air-driven reverse Brayton cycle, illustrated in Figure 3. It absorbs heat from the aircraft's internal cooling cycle (thermal transport bus – TTB) at lower temperatures (q_{TTB}) and releases it into the engine bypass flow at higher temperatures (q_{Byp}) through a bypass heat exchanger. Assuming adiabatic compression and expansion (specific work w_C , and w_T) the thermal output is calculated as $q_{BVD} = q_{TTB} + (w_C - w_T)$, where q_{TTB} represents the specific heat absorbed from the electrical systems (see Figure 3). This thermodynamic cycle inevitably necessitates additional (electrical) power \dot{W}_c to operate the compressor, which is supplied by the main engine through a generator connected to the high-pressure shaft. The additional power offtake reduces engine performance, resulting in increased fuel burn during a flight mission. Additionally, the presence of the heat exchanger in the bypass duct causes a pressure loss, which also negatively affects engine performance.

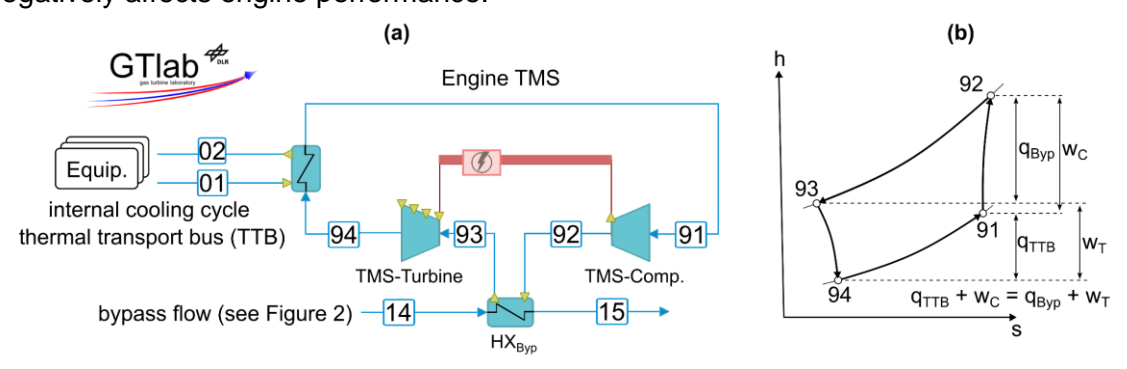


Figure 3 – (a) thermodynamic performance model of the engine-integrated TMS, (b) corresponding hs diagram.

The thermodynamic simulation is conducted using the modular software environment GTlab. The compressor and turbine of the TMS are modeled in analogy to the turbo components of the engine, utilizing appropriate component maps scaled to the design point to match specified design values. Off-design simulation is conducted according to the defined component maps.

The modeling of heat exchangers is carried out using the widely recognized P-NTU method [21]. The heat flow is defined as:

$$\dot{Q}_i = P_i \cdot C_i \cdot \Delta T_{max} \tag{1}$$

with
$$C_i = c_{p,i} \cdot W_i$$
 (2)

$$\Delta T_{\text{max}} = T'_2 - T'_1 \tag{3}$$

$$\Delta T_{max} = T'_2 - T'_1$$

$$P_i = \frac{\Delta T_i}{\Delta T_{max}} = \frac{|T'_i - T''_i|}{\Delta T_{max}}$$
(3)

' = in; " = out; assuming $T_2 > T_1$

The dimensionless temperature change P_i (also referred as effectiveness) is positively defined and represents the ratio of the temperature increase or decrease of a fluid to the maximum possible temperature change. This ratio is used to calculate the "number of transfer units" (NTU), a dimensionless transfer capability, in a heat exchanger. It quantifies the relationship between the heat transfer capability and the fluid capacity rate C_i , essentially comparing the heat exchange capacity with the energy required to change the temperature of the fluid by one Kelvin.

$$NTU_i = \frac{1}{1 - R_i} \cdot ln\left(\frac{1 - R_i \cdot P_i}{1 - P_i}\right) \text{ (countercurrent flow, } R \neq 1)$$
 (5)

$$NTU_i = \frac{U \cdot A}{C_i} \tag{6}$$

$$R_i = \frac{W_i}{W_i} \tag{7}$$

Off-design methodology

The thermodynamic cycle is modeled according to the following scheme: At the TMS design point, the pressure ratio of the TMS compressor Π , mass flow rates (W_{TMS} and W_{TTB}), the inlet temperature T_{01} of the TTB and the desired temperature reduction $\Delta T = T_{01} - T_{02}$ are specified. For the heat exchanger at the TTB, an effectiveness on the cooling medium side $P_{TTB} = 0.8$ is set. This indirectly specifies the required inlet temperature T_{94} . The bypass temperatures T_{14} are determined by the engine performance simulation. Given the specified TMS pressure ratio Π and the cycle closure conditions, the heat dissipated in the bypass heat exchanger \dot{Q}_{Byp} and its effectiveness P are subsequently determined.

Additionally, a simplified estimation is used to approximate the required size of the bypass heat exchanger, which in turn affects the mass flow (W_{14}) and consequently the capacity flow on the bypass side. This estimation is based on the calculated transfer area A and an assumed heat transfer surface density of $\beta = 500 \text{ m}^2/\text{m}^3$ [22], from which the volume (A/β) of the heat exchanger is determined. The entrance area (height * width) of the heat exchanger is then calculated using an assumed length of 0.5 m and a constant height of 0.14 m (maximum bypass height and length derived from the geometric predesign of the engine). The proportion of this entrance area A_0 relative to the total bypass area A_{Byp} corresponds to the proportion of the mass flow through the heat exchanger W_{14} relative to the total mass flow W_{12} (see Figure 2). This straightforward approach, which requires an iterative calculation of the bypass split ratio HX_{split} , allows for establishing a relationship between the heat exchanger geometry and the thermodynamic cycle. It also relates the pressure loss in the bypass to the size of the heat exchanger.

In off-design conditions, the system with its predefined heat exchangers responds to altered boundary conditions in the bypass duct. Consequently, the heat exchanged and temperature levels are a result of these changes, with the inlet temperature and mass flow in the TTB assumed to be constant and therefore not deviating from the design point. The system allows different control methods for the shaft speed and power of the TMS compressor. During the studies, the adjustment of the TMS mass flow under the condition of constant compressor power \dot{W}_c and speed ($N_{rel} = 1.0$) of the turbo components was identified as a suitable solution after an analysis of the component maps. The maps used are generic radial compressor and turbine maps from the GTlab database. It is conceivable that, depending on specific heat dissipation requirements and detailed maps, more suitable control methods for the TMS at off-design conditions could be identified. A summary of the design and off-design methodology is illustrated in Figure 4.

Design methodology

inputs W_{TTB} , T_{01} , ΔT_{TTB} , P_{TTB} off-design cycle matching: calc. req. T₉₄ W_{TMS} C_i results α, β, HX_{TTB} design design A calc. ΔT_{TMS} , ΔT_{TTB} **PLC** iterative calc. A $(P_{TMS}, \dot{Q}_{TTB}, ...)$ T₉₁, p₉₁ T₉₁, p₉₁ Π, η, $(N_{rel} = 1.0)$ compressor design design W_c compressor off-design Map T_{92} , p_{92} HX_{Byp} design T₉₂, p₉₂ initial HX_{split} α, β, iterative calc. A design A PLC calc. ΔT_{TMS} , ΔT_{Byp} HX_{split} sizing of HX $(\overline{P_i}, \overline{Q}_{Byp},...)$ A_0 I, h calc. of HX_{split} A_{Byp} T_{93} , p_{93} match HX_{split} $T_{93},\,p_{93}$ turbine design Мар turbine off-design match T₉₄, p₉₄

Figure 4 – design and off-design methodology of the engine-integrated TMS.

In these studies, Dow SYLTHERM 800 [23] is used as the cooling medium in the TTB. The overall heat transfer coefficient for both heat exchangers is assumed to be $U = 50 \text{ W/m}^2\text{K}$, a typical value for plate heat exchangers [21]. The mass of the heat exchanger is estimated using an assumed wall thickness of 0.5 mm and aluminium as the material ($\rho = 2700 \text{ kg/m}^3$), calculated using the formula $M_{HX} = A \cdot 0.5 \text{ mm} \cdot 2700 \text{ kg/m}^3$. The pressure loss coefficient ($PLC = p_{out}/p_{in}$) at the design point for both sides of the heat exchangers is estimated to be 0.96. In off-design conditions, the pressure loss varies depending on the pressure difference at design, changes in dynamic viscosity, average density and mass flow as modeled in [24].

5. Results and Discussion

Following the outlined design methodology, an engine-integrated TMS is developed and compared under different operating conditions. The cooling medium is initially assumed to enter the heat exchanger HX_{TTB} at a constant temperature of $T_{01} = 300$ K. The system is designed for maximum cooling performance, aiming to lower the coolant temperature to $T_{02} = 235$ K, resulting in a temperature difference of $\Delta T_{TTB} = 65$ K. The highest cooling potential is expected at an operating point where the heat sink (bypass duct) has favorable cooling properties, identified at the lowest temperatures of $T_{Byp} = 330$ K during the Patrol segment when the engine is operating at 35 % of maximum dry thrust. This point is set as the design point for the closed-air cycle. The mass flow in the TTB is initially set to 0.256 kg/s, achieving a design cooling flow of $\dot{Q}_{TTB} = 25$ kW. Assuming approximately equal capacity flows C_i ($c_{p,TTB} \approx 1.5 \cdot c_{p,air}$) in the HX_{TTB} , a design mass flow in the TMS of $1.5 \cdot W_{TTB} = 0.384$ is defined. The compressor pressure ratio is set to $\Pi = 8$ and will be varied in the following section. The remaining design parameters and resulting values are shown in Figure 5a.

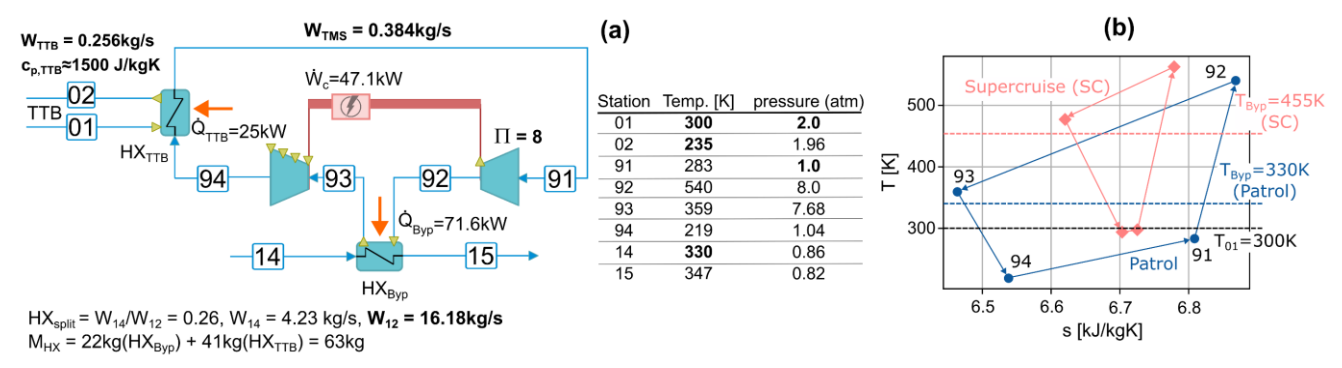


Figure 5 – **(a)** summary of design parameters (indicated by bold values) and resulting values for the engine-integrated TMS, referred as baseline design (BD) in the following figures. The TMS is designed for the Patrol segment with low bypass temperatures, **(b)** TS diagram for the chosen design point (Patrol) and supercruise.

Based on the chosen design, an analysis of the CAP flight mission is carried out. Figure 6a depicts how the cooling performance varies with flight duration, influenced by the prevailing bypass temperatures. During the Take-Off and Turn1 segments, temperatures exceed $T_{Byp} = 460 \text{ K}$, preventing the system from dissipating heat due to the excessively warm heat sink. Nevertheless, the average cooling performance is maintained at 23.2 kW, achieving 93 % of the designated design value across the entire mission.

Figure 6b shows the impact of the TMS on engine performance, specifically the amount of additional fuel required compared to a baseline configuration without TMS. The results demonstrate that the negative effect of the pressure loss Δp_{Byp} in the bypass is completely compensated by the heat introduced \dot{Q}_{Byp} . The main factors responsible for the higher fuel consumption are the required compressor power \dot{W}_c for the TMS as well as the additional mass of the heat exchangers M_{HX} , which necessitate higher thrust levels.

Figure 6c examines how scaling mass flows (W_{TMS} and W_{TTB} scaled proportionally) affects the resulting cooling performance and its impact on fuel consumption during the CAP mission. In fact, the mean heat dissipation \overline{Q}_{TTB} , the required TMS compressor power \dot{W}_c and the mass of the heat exchangers M_{HX} change proportionally to the mass flow rate. While the additional fuel requirement remains acceptably low at less than 3 %, the size of the heat exchanger in the bypass significantly

increases. For a mean cooling flow of \overline{Q}_{TTB} = 44 kW, the heat exchanger already takes up 50 % of the bypass. This suggests that the maximum amount of heat that can be dissipated by an engine-integrated TMS is dependent on the maximum size of the heat exchanger and its integration into the bypass.

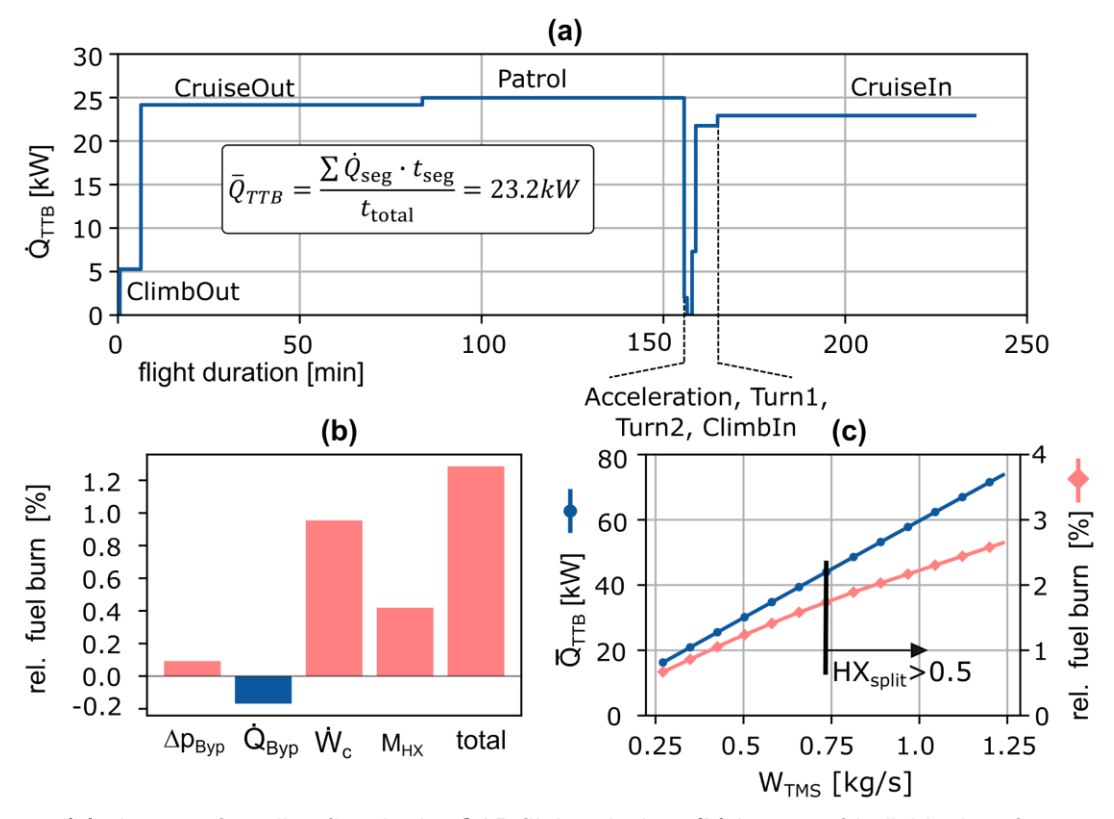


Figure 6 – (a) change of cooling flow in the CAP flight mission, (b) impact of individual performance changes due to the TMS on the relative fuel burn in the CAP flight mission, (c) changes of mean cooling flow and relative fuel burn for a variation of the air flow in the TMS and TTB (scaled proportionally).

The significant decrease in cooling performance at high-load operating points is highlighted in Figure 5b using a TS diagram. Alongside the Patrol design point, cycle parameters for supercruise conditions are also displayed. The system requires the exit temperature from the bypass heat exchanger, T_{93} , to be lower than the bypass inlet temperature, T_{Byp} . Moreover, heat absorption in the HX_{TTB} necessitates a cooler exit temperature $T_{91} < T_{01} = 300$ K. The TS diagram shows that at high bypass temperatures, cooling performance and system efficiency (e.g., coefficient of performance, COP) significantly decrease. This issue is particularly problematic during extended high-performance flight phases, such as long supercruise segments. In shorter high-performance segments, like those included in the CAP mission, the engine's lower cooling capacity may be compensated by additional cooling systems (e.g., ram-air or fuel cooling). It can be assumed that the low cooling capabilities in these high-load operating points are the cause of the decreasing performance of modern fighters, as significantly lower amounts of heat can be dissipated and systems may overheat as a result. The challenge is therefore to identify suitable solutions for demanding flight maneuvers with high bypass temperatures T_{Byp} . Possible approaches are discussed in the following sections as part of the variations of various TMS design parameters.

5.1 Variation of TMS pressure ratio

Next, a variation of the TMS compressor pressure ratio Π at the design point is analyzed. Changes in selected objectives are shown in Figure 7. The given values are relative to the presented baseline design (BD) in Figure 5. Increasing the pressure ratio raises the temperature difference at the heat exchanger entries $\Delta T_{TMS} = T_{92} - T_{94}$. Since T_{94} is defined by the required cooling flow \dot{Q}_{TTB} , the heat exchanger effectiveness P_{TTB} and cooling medium temperature levels ΔT_{TTB} , the inlet temperature into the bypass heat exchanger T_{92} is increased, see TS diagram in Figure 7b. This higher

PERFORMANCE ASSESSMENT OF AN ENGINE INTEGRATED CLOSED-AIR THERMAL MANAGEMENT SYSTEM

temperature improves heat transfer in the bypass, making it smaller and lighter. As a result, the required entrance area A_0 decreases, reducing pressure loss in the bypass. Moreover, the heat added in the bypass increases with the pressure ratio, positively impacting engine performance. However, higher pressure ratios also demand more compressor power \dot{W}_c , which must be provided by the engine, reducing overall engine performance. For the selected design and the given DLR-FFD configuration, these opposing effects are approximately balanced so that fuel consumption within the CAP mission is nearly constant at different pressure ratios.

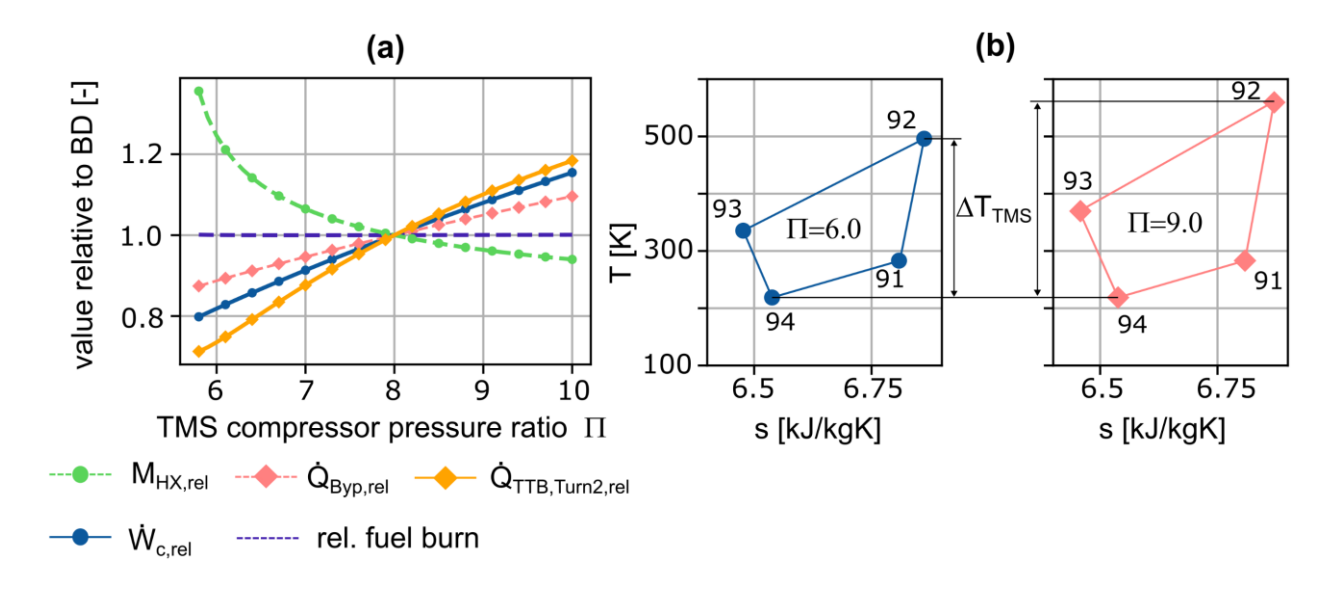


Figure 7 – (a) change of relative quantities for a variation of the TMS compressor pressure ratio Π , (b) comparison of TS diagrams for compressor pressure ratios Π = 6 and Π = 9.

At a TMS compressor pressure ratio below 5.8, a thermodynamic limit is reached due to insufficient temperatures T_{92} , where the bypass heat exchanger exit temperature T_{93} would need to exceed the theoretically possible maximum temperature in the bypass T_{Byp} (effectiveness $P_{TMS} > 1.0$). It's worth noting that counterflow heat exchangers can achieve effectiveness close to 1, while other types, like crossflow, may reach significantly lower values. This case is an optimistic assumption and indicates that high pressure ratios $\Pi > 5.8$ are necessary at the chosen temperature levels ΔT_{TTB} combined with the range of bypass temperatures T_{Byp} of the DLR-FFE.

Higher pressure ratios in the TMS lead to increased temperature differences in the air cycle ΔT_{TMS} , enhancing cooling capability at high-load operating points. Figure 7a illustrates how cooling performance changes in the Turn2 segment, suggesting that high pressure ratios are generally desirable as their benefits outweigh the additional power requirements of the TMS compressor. However, the pressure ratio is already high compared to typical air cycle machines (ACM), which usually achieve pressure ratios of 2-3 with single-stage turbo components [25]. Implementing such systems poses additional design challenges, potentially necessitating two compressors and turbines, increasing complexity, pressure losses and total system weight. Detailed component knowledge and design considerations are essential for setting an appropriate pressure ratio. In future studies, more sophisticated methods will be employed to account for the design of the TMS turbo components, including an estimation of their size and weight. This approach aims to integrate these factors more comprehensively into the overall design process of TMS solutions.

Thermodynamically, changes in absolute pressure levels in the TMS have a negligible impact when pressure ratios remain constant, only slightly affecting gas properties such as specific heat capacity. However, the absolute pressure is crucial for the practical implementation of the system. For example, the wall thickness of the heat exchanger transfer surface is usually determined by the maximum pressure difference between the fluids. In addition, the absolute pressure level is important in the design of turbomachinery components since it affects their efficiencies and operating behavior.

5.2 Variation of TMS mass flow

Subsequently, the mass flow in the air cycle is varied while keeping the design cooling flow $\dot{Q}_{TTB} = 25$ kW requirement constant. This tests the initial assumption of approximately equal capacity flows ($C_{TMS} \approx C_{TTB}$) at the design point. The behavior of selected objectives is illustrated in Figure 8a. Increasing the mass flow in the air cycle, while maintaining the same required heat transfer \dot{Q}_{TTB} , results in a reduced temperature change in the heat exchangers according to $\dot{Q}_{TTB} = W \cdot c_p \cdot \Delta T$. This leads to a reduced overall temperature difference in the TMS ΔT_{TMS} , which in turn results in a reduction in cooling performance at off-design conditions, especially at high-load operating points, similar to the effect described for a variation of the TMS pressure ratio in Section 5.1. Changes in cooling flow for the Turn2 segment are illustrated in Figure 8a. While the compressor power \dot{W}_c increases as expected with rising mass flow, the required transfer area A in the HX_{TTB} decreases according to the P-NTU method, thereby reducing its weight. Overall, fuel consumption remains approximately constant. Nevertheless, lower mass flows, which provide higher temperature differences in the TMS, are generally preferred for improved cooling potential under off-design conditions. However, a physical limit is reached when mass flows are too low and the air cycle must be heated above the TTB entry temperature, T_{O1} , to transfer the required heat (effectiveness P > 1.0).

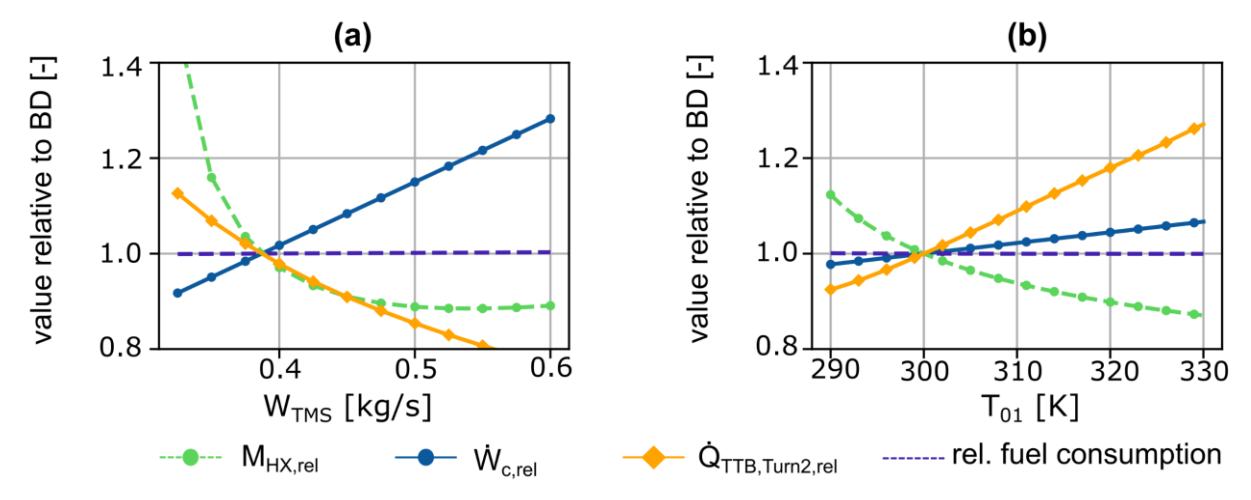


Figure 8 – (a) change of relative quantities for a variation of TMS air cycle mass flow and (b) cooling medium inlet temperature in the TTB.

5.3 Variation of TTB temperatures

Finally, this section discusses variations in the selected design values in the TTB. Previous sections have established that high temperature differences ΔT_{TMS} are generally preferable due to their positive impact on off-design cooling performance. Variations of the temperature change in the TTB have shown that higher temperature differences ΔT_{TTB} are generally preferred, as they also result in larger temperature changes within the TMS. Therefore, the following analysis focuses on the influence of the inlet temperature T_{01} while maintaining a constant temperature reduction ($\Delta T_{TTB} = 65$ K). The results are illustrated in Figure 8b. Each design was set to achieve the required cooling flow of $\dot{Q}_{TTB} = 25$ kW for the Patrol segment.

Raising the inlet temperature T_{01} generally increases the cooling potential across the operational range, as demonstrated by the heat dissipation in the Turn2 segment. Higher TTB inlet temperatures T_{01} lead to higher HX_{TTB} exit temperatures in the TMS, T_{91} , resulting in higher temperature levels at the compressor exit T_{92} for the same pressure ratio. This enhances the cooling potential in high-load operating points with hotter bypass temperatures. Additionally, higher inlet temperatures in the bypass heat exchanger T_{92} reduce the required transfer surface area A, resulting in more compact and lighter heat exchangers, while the required compressor power \dot{W}_c increases only slightly. It's important to note that the inlet temperature of the coolant is usually defined by the systems being cooled and the properties of the cooling medium, and cannot be arbitrarily increased. However, the results highlight the thermodynamic benefits of warmer inlet temperatures T_{01} .

6. Conclusion

This paper presents an engine-integrated TMS utilizing a closed-air reverse Brayton cycle to transfer heat from the coolant in a thermal transport bus of electrical systems to a military engine's bypass flow. Utilizing existing fighter and engine configurations from previous DLR studies, performance simulations were conducted to examine operation during a flight mission, focusing on cooling capability and effects on engine performance as well as fuel consumption. Key findings include:

- Fuel consumption increases mainly due to the additional power required by the TMS
 compressor and the mass of the heat exchangers. The negative effects of the pressure loss
 in the bypass duct due to the heat exchanger are negligible and generally compensated by
 the positive effect of the additional heat input.
- While the increase of fuel consumption is acceptably low, the maximum cooling flow is limited by the size of the bypass heat exchanger.
- Generally, high temperature changes in the air cycle are preferable to maintain cooling potential at higher bypass temperatures. This can be achieved through high pressure ratios in the TMS compressor. In addition, the mass flow should be selected in such a way that high temperature changes are achieved in the heat exchangers.
- The cooling capability increases as the temperature of the cooling medium approaches the bypass temperature. Thermodynamically, colder bypass temperatures and warmer coolant inlet temperatures are preferred.

The primary challenge identified is ensuring cooling performance at high-load operating points with high bypass temperature levels. This fact clearly demonstrates that for an efficient application of engine-integrated TMS, it is advisable to combine it with an engine in which a cold bypass channel with continuous flow prevails even at high-load. In this context, variable cycle engine (VCE) architectures with an additional external bypass channel offer significant advantages. Future studies will investigate the combination of the given fighter configuration with such a propulsion system and an integrated TMS and evaluate its benefits compared to the presented conventional architecture.

7. Copyright Statement

The authors confirm that they, and/or their company or organization, hold copyright on all of the original material included in this paper. The authors also confirm that they have obtained permission, from the copyright holder of any third party material included in this paper, to publish it as part of their paper. The authors confirm that they give permission, or have obtained permission from the copyright holder of this paper, for the publication and distribution of this paper as part of the ICAS proceedings or as individual off-prints from the proceedings.

References

- [1] Jafari, S. and Nikolaidis, T. *Thermal Management Systems for Civil Aircraft Engines: Review, Challenges and Exploring the Future.* Appl. Sci. 8(11)2044, 2018.
- [2] Dooley, M., Lui, N., Newman, R., and Lui, C., *Aircraft Thermal Management -Heat Sink Challenge* SAE Technical Paper 2014-01-2193, 2014.
- [3] van Heerden, A.S.J., Judt, D.M., Jafari, S., Lawson C.P., Nikolaidis T. and Bosak, D. *Aircraft thermal management: Practices, technology, system architectures, future challenges, and opportunities.* Progress in Aerospace Sciences, Vol. 128, 2022.
- [4] Iden, S., Sehmbey, M., and Borger, D., *MW Class Power System Integration in Aircraft*. SAE Technical Paper 2004-01-3202, 2004.
- [5] Warwick, G. New AFRL Program Focuses on Aircraft Energy Issues. Aviation Week &Space Technology, vol. 172, no. 25, 2010.
- [6] Ganev, E. and Koerner, M. Power and Thermal Management for Future Aircraft. SAE 13ATC-0280, 2013.
- [7] Thompson, L. *Inside Block 4 The Mostly Secret Plan For Making The F-35 Fighter Even More Lethal.* online available: https://www.forbes.com/sites/lorenthompson/2022/11/14/inside-block-4-the-mostly-secret-plan-for-making-the-f-35-fighter-even-more-lethal/, 2022.
- [8] Losey, S. *The F-35 engine is at a crossroads, with billions of dollars for industry at stake.* online available: https://www.defensenews.com/air/2022/07/15/the-f-35-engineis-at-a-crossroads-with-billions-of-dollars-for-industry-at-stake/, 2022.
- [9] Marrow, M. It's official: The F-35 will not get a new engine anytime soon. online available:

PERFORMANCE ASSESSMENT OF AN ENGINE INTEGRATED CLOSED-AIR THERMAL MANAGEMENT SYSTEM

- https://breakingdefense.com/2024/03/its-official-the-f-35-will-not-get-a-new-engine-anytime-soon/, 2024.
- [10]Clark, R. A Method for the Conceptual Design of Integrated Variable Cycle Engines and Aircraft Thermal Management Systems. Ph.D. dissertation, Georgia Institute of Technology, 2023.
- [11]Lin, Y.R., Kota K., Chow, L.and Leland, Q. Design of a Thermal Management System for Directed Energy Weapons, 2009.
- [12]Gvozdich, G., Weise, P. and von Spakovsky, M. *INVENT: Study of the Issues Involved in Integrating a Directed Energy Weapons Subsystem into a High Performance Aircraft System.* 50th AIAA Aerospace Sciences Meeting, 2012.
- [13]Donovan, A., Nuzum, S., Roberts, R., and Wolff, M. *Impact of High Energy Pulsed Systems on an Aircraft's Power and Thermal Management System*, AIAA SciTech, 2016.
- [14]Maser, A. Optimal Allocation of Thermodynamic Irreversibility For The Integrated Design of Propulsion and Thermal Management Systems. Ph.D. dissertation, Georgia Institute of Technology, 2012.
- [15]Clark, R. A., Shi, M., Gladin, J., and Mavris, D. Design and Analysis of an Aircraft Thermal Management System Linked to a Low Bypass Ratio Turbofan Engine. ASME. J. Eng. Gas Turbines Power, 2022.
- [16]Clark, R. A., Tai, J., and Mavris, D. *Integrated Design of a Variable Cycle Engine and Aircraft Thermal Management System.* ASME. J. Eng. Gas Turbines Power, 2024.
- [17]Liersch, C.M, Schütte, A, Moerland, E. and Kalanja, M. *DLR Project Diabolo: An Approach for the Design and Technology Assessment for Future Fighter Configurations*. American Institute of Aeronautics and Astronautics (AIAA) Aviation Forum, 2023.
- [18] Mancini, A., Zamboni, J. and Moerland, E. *A knowledge-based methodology for the initiation of military aircraft configurations*. American Institute of Aeronautics and Astronautics (AIAA) AVIATION Forum, 2021.
- [19]Matuschek, T., Otten, T., Zenkner, S., Becker, R., Zamboni, J., and Moerland, E. *Application of a Multidisciplinary Design Process to Assess the Influence of Requirements and Constraints on the Design of Military Engines*. ASME. J. Eng. Gas Turbines Power. 2024.
- [20]Reitenbach, S., Becker, R., Hollmann, C., Wolters, F., Vieweg, M., Schmeink, J., Otten, T., and Siggel, M. *Collaborative Aircraft Engine Preliminary Design using a Virtual Engine Platform, Part A: Architecture and Methodology.* AIAA SciTech Forum, 2020.
- [21]Stephan, P., Kabelac, S., Kind, M., Mewes, D., Schaber, K. and Wetzel, T. *VDI-Wärmeatlas mit 1046 Abbildungen und 483 Tabellen.* 12. Auflage, Springer Vieweg, p.39-97, 2019.
- [22] Shah, R.K. and Sekulic, D.P. Fundamentals of Heat Exchanger Design, Classification of Heat Exchangers. John Wiley & Sons, Inc., p.1-77, 2003.
- [23]The Dow Chemical Company, 1997, SYLTHERM 800 Heat Transfer Fluid. The Dow Chemical Company, online available, https://www.dow.com/content/dam/dcc/documents/en-us/app-tech-guide/176/176-01435-01-syltherm-800-heat-transfer-fluid.pdf, pp. 1–28, 2024.
- [24]Nöske, F.T. Modellierung und Bewertung des Off-Design Verhaltens von Verdampfern in der Triebwerksvorauslegung. master thesis, Technische Universität Berlin, 2022.
- [25]Santos, A.P.P., Andrade, C. and Zaparoli, E. *A Thermodynamic Study of Air Cycle Machine for Aeronautical Applications*. International Journal of Thermodynamics 17(3):117-126, 2014.